Force Controlled Semi-active Damping in Vehicle Suspension Systems

by:

Clint Whitlock

University Undergraduate Fellow, 1993-1994

Texas A&M University

Department of Mechanical Engineering

APPROVED

Fellows Advisor Rob Redfield

Honors Director

OVERVIEW

Negative feedback control is a concept that dates back to antiquity. Nevertheless, the microprocessors, actuators, and sensors required to implement various control strategies have only recently become inexpensive enough to be viable components in many applications. Consequently, many dynamic systems whose performance could be considerably improved with the addition of some type of control strategy are operating at sub-optimal levels of performance. Because of the recent huge technological advances which have acted to drive down the cost of these feedback system components and the growing field of controls study, new applications are being found continually which lend themselves nicely to control via negative feedback. One such application that has recently received a lot of attention from both academic and commercial groups is the automobile suspension system.

To present, vehicle suspension systems have been designed integrating completely passive devices to obtain the desired results for certain predetermined performance criteria. Those criteria might include average suspension travel (stroke), vehicle body acceleration, and tire - road contact force, as well as others. Because of the strictly passive nature of the components that make up the suspension system, previous efforts at suspension design have been guided by a bias toward a particular performance criterion. Open loop system design necessarily prioritizes those performance criteria according to the vehicle's primary application. Consequently, increased performance in one criterion necessarily comes at the expense of decreased performance from another design viewpoint, both of which have a focused purpose and application. For example, a sports car may be designed with an emphasis on handling performance, so road holding would be prioritized above and at the expense of vehicle body acceleration. Likewise, a luxury sedan would be designed with a bias toward ride comfort and so road holding and suspension travel would be prioritized below vehicle body acceleration. In both of these cases, performance from one design viewpoint is maximized with less regard to the implications this maximization has upon other design variables.

The passive devices previously used in suspension systems have included exclusively

compliant (modeling that of a spring) and dissipative (modeling that of a damper) components, both of whose characteristics were fixed. Recently, commercial and academic interest has been devoted to the study of the performance of vehicle suspension systems upon the addition of active damping, where a controlled force is provided between the vehicle wheel and body based on measured performance variables (Redfield and Karnopp, 1988), and some semi-active damping, where an electrically controlled component acts to dissipate energy only while no force requiring the addition of power to the component is needed (Redfield 1990). Such devices, if implemented, could lend to the greater optimization of all performance measures to a certain extent.

The intrinsic worth of closed loop feedback control lies in the fact that, if chosen correctly, a control scheme can optimize, or at least, improve upon the dynamic response of a particular system to a specified input. Several different control strategies have been proposed for implementation into the the design of suspension systems. The various strategies can be categorized for the most part by the mechanism in which power is dissipated from the system. In active damping (Crosby and Karnopp, 1973), the optimization is realized through an electrically controlled component which has the ability to sense instantaneous performance measures in a dynamic situation and in turn, provide a force that will optimize the performance of the suspension system. The drawbacks to such an element are the large amounts of power that must be delivered to the system, the increased complexity of the system, and the loss in reliabity of system performance.

An alternate approach that reaps some of the same advantages that the active damper lays claim to can be obtained with a semi-active damper (Karnopp, 1974). The term "semi-active" can be somewhat misleading because the added component is still completely passive, that is, it remains a dissipative control, but its behavior is controllable. The advantage here lies in the fact that relative to the active damper, inconsequential amounts of power are needed for the electrical control of the semi-active damper. In application, the semi-active damper "deactivates" when the addition of power to the system would be required to produce a force in order to dissipate energy. However, it does act to dissipate energy when the actuator finds that energy needs to be passively

removed from the system for optimal operation.

The purpose of this paper is to examine the effects of a force controlled semi-active damping scheme on various suspension performance criteria. The first section is devoted to the development of a mathematical model for purposes of dynamic analysis. Also included is a brief introduction to three basic control laws, culminating in the introduction of force controlled semi-active damping. Results of a computer simulation of the dynamic performance of a vehicle suspension system with a force controlled semi-active element concludes the section. The second section of the paper is a detailed explanation of an experimental test rig and data acquisition procedure that may be used to verify experimentally the results obtained through computer simulation of the same control strategy.

Part 1

THE MODEL

To specify each of the generalized coordinates and write all of the equations of motion necessary to fully describe the dynamics of an automobile would indeed be a cumbersome task. An even greater task still would be trying to gain some insight as to the effects of different control schemes on certain performance criteria with a model of such mathematical complexity. An alternative approach in studying the dynamics of a vehicle suspension system is to look at the quarter car model shown schematically in Fig. 1. This two degree-of-freedom model is much simpler to analyze mathematically, and it still preserves the essence of the dynamics of the system.

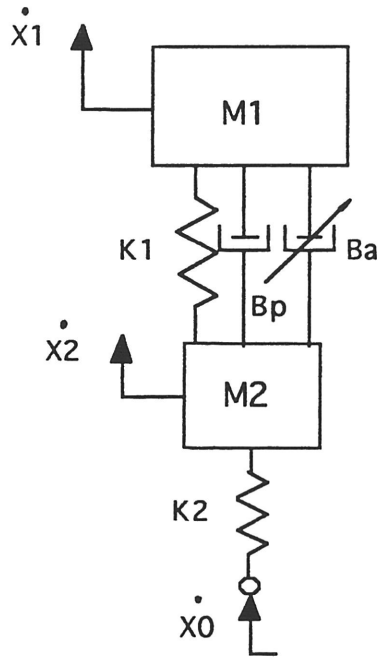

Fig. 1. Schematic of quarter car model

Consequently, results obtained with this quarter car model are much more meaningful intuitively and there is much less room for error in computation. The large mass **M1** respresents the mass of the vehicle body, or the sprung mass. The smaller mass **M2** represents the mass of the wheel and will be termed the unsprung mass. Compliances **K1** and **K2** model the stiffness of the suspension and the stiffness of the tire, respectively. The damping coefficient **Bp** respresents the passive damping characteristic of the suspension while the coefficient **Ba** represents the variable controlled damping. As its name implies and is evident from the schematic, one quarter of the vehicle is modeled with this scheme so the only degrees of freedom considered are the vertical displacements of masses **M1** and **M2** which are represented in the schematic by the velocities $\dot{\mathbf{X}}\mathbf{1}$ and $\dot{\mathbf{X}}\mathbf{2}$ respectively. The difference in these two velocities, namely $\dot{\mathbf{X}}\mathbf{1} - \dot{\mathbf{X}}\mathbf{2}$, will be referred to as **Vrel** , the relative velocity across the suspension system. The input to the system is represented by an input velocity $\dot{\mathbf{X}}\mathbf{0}$, which represents the effect of changes in roadway profile at a specific vehicle forward velocity. A discussion of such roadway profile generation is included later in the section.

With the fully defined model, the equations of motion for the quarter car system can be expressed in state variable matrix form as in equation (1) below. The variables **X1** and **V1** represent the position and velocity,

$$\frac{d}{dt}\begin{bmatrix} X1 \\ V1 \\ X2 \\ V2 \end{bmatrix} = \begin{bmatrix} 0 & 1 & 0 & 0 \\ \frac{-K1}{M1} & \frac{-DC}{M1} & \frac{K1}{M1} & \frac{DC}{M1} \\ 0 & 0 & 0 & 1 \\ \frac{-K1}{M2} & \frac{-DC}{M2} & \frac{-(K1+K2)}{M2} & \frac{-DC}{M2} \end{bmatrix} \begin{bmatrix} X1 \\ V1 \\ X2 \\ V2 \end{bmatrix} + \begin{bmatrix} 0 \\ 0 \\ 0 \\ \frac{-K2}{M2} \end{bmatrix} X0 \qquad (1)$$

respectively,of **M1**, while **X2** and **V2** represent the position and velocity of **M2**. Also, the **DC** term in the equations of motion represent the applicable damping coefficient depending on the damping control strategy being studied. For today's typical automobile, there is only a passive damping coefficient, and thus the total damping coefficient in the expression would take on the value of **Bp** only. As represented in Fig. 1, the controlled damper, **Ba** is variable in nature and can take on a range of values as will be shown later. For the present analysis, a typical commercially available suspension will be used in which the value of **Ba** would effectively be zero.

Average component values for today's typical vehicle suspension system as used in suspension research (Karnopp, 1983 and Redfield, 1989) are shown below.

Table 1. Vehicle Suspension Parameters

Component	Value
M1	267 kg
M2	36.6 kg
K1	18,400 N/m
K2	187,000 N/m
Bp	1398 N • s/m

MODEL ANALYSIS

In order to obtain a feel for the dynamics of the quarter car model being investigated, a detailed analysis of the model was carried out. First, from the matrix form of the equations of motion listed above in the form

$$\dot{x} = \mathbf{A}\cdot x + \mathbf{B}\cdot u \qquad (2)$$

the **A** matrix was analyzed for the system eigenvalues and the results plotted in the s-plane as shown in Fig. 2. The eigenvalues for the model with the damping coefficient equal only to the passive damping value were the two complex conjugate pairs

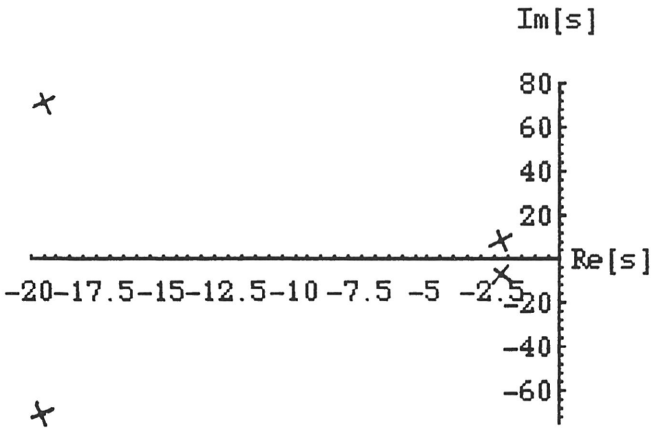

Fig. 2. Pole placement for passive damping

$$s_{1,2} = -19.5036 \pm 70.6379j$$

$$s_{3,4} = -2.21274 \pm 7.8914j$$

As seen in Fig. 2, both sets of complex conjugate pairs fall in the left half plane, which corresponds to a condition of stability for both sets of eigenvalues. The natural frequencies of the two different responses are about 8 and 73 rad/s, or 1 and 10 Hz. The faster natural frequency corresponds to that of the wheel mass which is on the order of one magnitude greater than that of the sprung mass. The larger frequency response (i.e., the faster dynamic response) will be the dominant response in determining the data acquisition rates for purposes of dynamic simulation. Also, with an idea of the active dynamic range for the suspension system, a proper roadway elevation profile can be created.

CONTROL STRATEGIES

Several different control strategies suitable for application in vehicle suspension systems have been researched and documented in dynamic controls literature. The various control

strategies can, for analytical purposes, be classified into one of three groups, depending upon the type of damping present in the suspension system.

For the first case, consider the typical commercially available suspension system. To present, the vast majority of automobiles sold to the public have consisted of purely passive suspension systems. In order to understand what is implied by a purely passive component, an examination of the constitutive relationship between force and relative velocity across a damper is necessary. Fig. 3 shows that constitutive relationship for a linear damper, or one in which the relationship between the force and relative velocity across the damper is constant. The interpretation of this relationship is that with a completely passive damping element, energy can only be dissipated from the system as is evidenced from the fact that the relation only holds in the first and third quadrants. If an extension of the damper is considered to be a positive relative velocity across the damper, then a force opposing this expansion, or a tensile force (considered positive) will be provided by the damper. Likewise, if the damper is being compressed, the relative velocity across the damper will be considered negative and a negative force, or a force opposing the compression of the damper will be provided. Because the relation only holds for the first and third quadrants, it is impossible to obtain a negative (compressive) force while the damper is expanding (positive relative velocity) or a positive (tensile) force while the damper is being compressed. The relation also shows that when there is no relative velocity across the damper, there is no force present. Also noticeable from the graph is that the slope of the line is equal to the damping coefficient of the linear passive damper. Thus, by varying the slope of this relationship, or effectively changing the damping coefficient, a stiffer or softer damper is represented depending on whether the slope is increased (stiffer) or decreased (softer). When the damping characteristic of the vehicle suspension system studied is characterized by the constitutive law presented above, the suspension is said to be purely passive in nature, or alternatively, this is open loop system design.

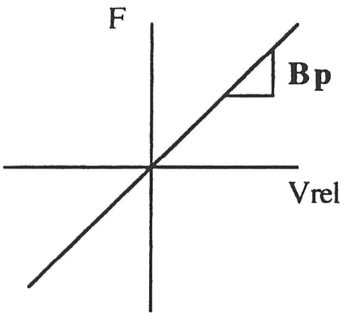

Fig. 3. Constitutive relationship for linear passive damper

At the other end of the spectrum of damping control strategies is a concept called active damping. Active damping is fundamentally different from passive damping in that the constitutive law between force and relative velocity for an active damper does in fact enter the second and fourth quadrants as shown in Fig. 4. A typical active damping scheme is achieved by applying a force proportional to the velocity of the sprung mass (**V1**) between the sprung and unsprung masses as represented by the schematic in Fig. 1. Now, instead of the suspension system being a purely passive system which dissipates energy only, the system must produce power to provide a force between the masses which is applied whenever conditions exist that shift the constitutive relation between relative velocity and force applied into the second and fourth quadrants. As seen from the relation in Fig. 4, with the active damper, there is still a characteristic slope which can be interpreted in the same way as in the passive case; that is, the slope represents the effective damping coefficient of the damping element. Now, however, there is another component in the damping equation, which can be written

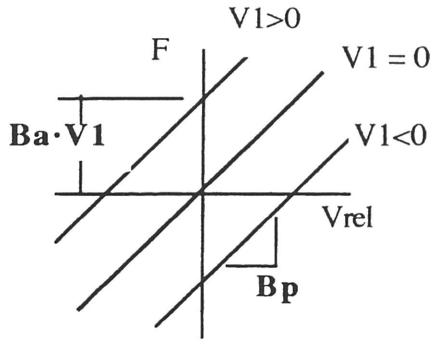

Fig. 4. Constitutive relation for passive plus active damping law

$$F_d = Bp \cdot Vrel + \underline{Ba \cdot V1} \quad (3).$$

where F_d is the total damping force. The underlined term in equation (3) compensates for the "active" nature of the damper in the damping force calculation. The physical interpretation of the underlined term is simply a shift of the damping law in the vertical direction of magnitude equal to the product of the active damping coefficient, **Ba**, and the velocity of the sprung mass, **V1**. Therefore, if the velocity of the sprung mass is positive, the shift in damping law will be vertically upwards while a negative sprung mass velocity will result in a downward vertical shift in the damping law.

Somewhere between the range of completely passive and completely active systems are semi-active systems. Semi-active systems can approximate the effectiveness of active systems when power is to be dissipated, without requiring the large amounts of supplied power and

extreme complexity that accompany active systems because of the necessary power production. Semi-active systems emulate the behavior of active systems when energy is being dissipated from the system, however when a damping force requiring the addition of power is experienced, the damping force is set to zero because the semi-active controller cannot supply power--only dissipate it. In other words, the semi-active system is active in the first and third quadrants, yet "shuts off", yielding a zero value of damper force when the damper operation enters the second or fourth quadrants. The constitutive law for what Redfield has termed "nominal" semi-active systems is represented in Fig. 5. As was the case for the active system, the slope of the semi-active damping law can be expressed as a passive damping coefficient, and any translation along the ordinate axis is equal in magnitude to the product of the active damping coefficient and the velocity of the sprung mass. Physically this "nominal" semi-active damping law says that when the damper is switching from tension to compression there exists discontinuities during the transition that correspond to times when the law enters the second and fourth quadrants. As a consequence of these discontinuities, the damper must switch with the change in sign of the relative velocity across the damper. The shortcoming of such a control strategy is the high frequency switching rate of the damper which is physically difficult to achieve. Solutions to this problem have been offered by Karnopp in the form of so called resistance controlled and force controlled semi-active damping (Karnopp, 1990). Both of these schemes achieve the same semi-active damping strengths while requiring a much lower active bandwidth. With resistance control, as shown in Fig. 6, the slope of the damping law is controlled, for example, by varying the size of an orifice in the flow path of the damper.

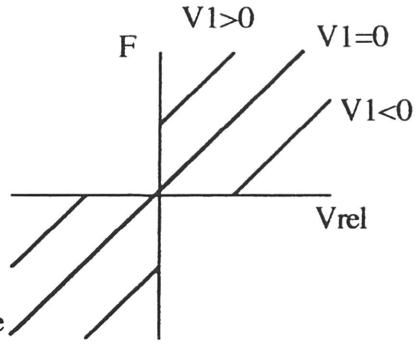

Fig. 5. "Nominal" Semi-active damping constitutive relationship

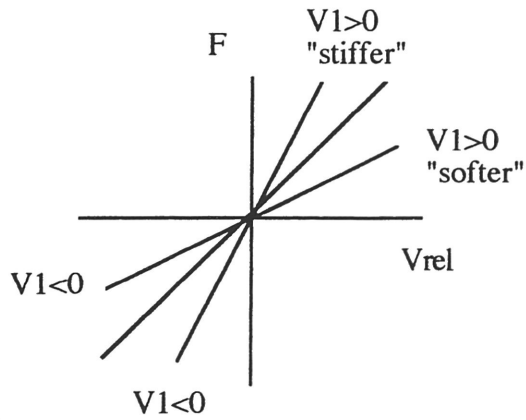

Fig. 6 - Resistance controlled semi-active damping

Inherent to this type of control is the fact that it allows for a much slower actuator because the slope of the damping law is changed in either the first or the third quadrant (not both), depending upon whether the sprung mass velocity is positive or negative.There is also no discrete jump along the ordinate axis at zero relative velocity as with other forms of semi-active damping. Instead the feedback from the system tends to "stiffen" or "soften" the damper by varying the resistance to fluid flow through the damper. For example, at times when more energy needs to be dissipated from the system, the flowpath is made smaller and the stiffer damper dissipates more energy. The opposite occurs when less energy needs to be dissipated from the system.

Force Controlled Semi-active damping

The emphasis of this paper will be on the application of a force controlled semi-active damping scheme. The control law for force controlled semi-active damping is shown in Fig. 7 and represented in equation (5) form below:

$$F_a = \begin{cases} Ba \cdot V1 & V1 \cdot Vrel > 0 \\ 0 & V1 \cdot Vrel \leq 0 \end{cases} \qquad (5)$$

In general, the semi-active control force is a function of both the relative velocity across the damper and the sprung mass velocity and has a value proportional to the sprung mass velocity with the proportionality constant being Ba, the active damping coeffieicient. The total suspension damping force is then equal to the semi-active control force in addition to the passive damping force (Bp·Vrel). Force controlled semi-active damping physically works as follows: If the relative velocity across the suspension is positive, which will be assumed for this explanation as an extension of the damper, and the velocity of the sprung mass is in the positive direction, an active force will be set equal in magnitude to the product of the active damping coefficient and the sprung mass velocity. There will be no relative velocity across the damper until the force applied across the damper reaches this

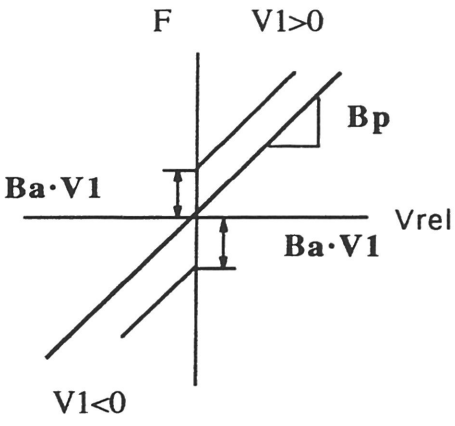

Fig. 7 - Force controlled semi-active damping

value, at which time there will be a relative velocity and then the total damping force becomes equal to the sum of both the active and passive contributions. This is the physical explanation of the shift of the damping law along the ordinate axis. Likewise, if the relative velocity across the suspension is negative (the suspension is being compressed), and the sprung mass velocity is negative, a total damping force will be supplied against the relative motion of the suspension system and can be calculated in an analagous manner to the above example. Here again, it should be noted that this control law, as does the resistance control, stiffens or softens the suspension in compression and tension separately, thus allowing for slower actuator operation. If the sprung mass velocity and the relative velocity across the suspension are of opposite sign, then the active nature of the damper "shuts off" and the damper emulates a passive element.

COMPUTER SIMULATION

In order to gain some insight into the types of forces produced within and the dynamic response of the quarter car model, several ACSL computer simulations were made. Perhaps the most critical information to be gained from the simulation was an idea of the magnitudes of the actuator forces required so that a proper linear actuator could be selected for use in the experimental test rig. Valuable also, was a look at the theoretical effect that varying values of the the active damping coefficient had on parameters such as the isolation of the sprung mass. With the equations of motion for the model already in hand, an idea of the dominant time constant for data acquisition purposes, and an equation form of the control law, the only component of the simulation left to be formulated was the roadway profile.

Road Profile Generation (Redfield and Karnopp, 1988)

Running a computer simulation to properly test the model prior to hardware setup requires some type of generated disturbance input to the model representative of the unevenness of a typical road. Before the exact procedure for obtaining a sample roadway is discussed, it is first necessary to define some of the nomenclature involved in the development. For simulation purposes Dodds

and Robson, 1973 used the notion that a roadway profile can be described as a Gaussian distribution of random roadway slopes. Redfield and Karnopp later showed that those slopes can be computed as a function of the natural frequency of the vehicle model, the desired range over which the spectral density remains relatively flat within a specified attenuation, and the vehicle forward speed. With these parameters set, the step-length of the road desired between slope changes and the standard deviation of those random slopes can be calculated. Finally, assuming an average slope of zero the roadway profile can be generated with slopes approximately "white" in frequency. Proper formulation of the road surface is essential because of the fact that roadways with greatly variable spectral densities have associated with them different levels of power input to the vehicle model. The basic concept behind a spectral analysis is that a signal (in this case the variation of the road slopes as a function of time) can be divided or decomposed into a set of pure waves, each with a characteristic wavelength. For instance, in the case at hand the roadway can be idealized as being made up of a number of waves with different wavelengths. The spectral density of any signal is a measure of the power carried by that signal within some small interval of wavelength (or frequency). That is, spectral densities carry different measures of power depending on the standard deviation, or more appropriately, the variance, of the amplitudes of the different wavelengths which make up the spectrum.

With a chosen roadway spectral density, Redfield and Karnopp showed that the process for obtaining the necessary step-length of the road between different slope values is straightforward. First, the zero frequency of the spectral density must be found. Then, values for the attenuation of that zero frequency can be chosen and the cutoff frequency at that attenuation can be found. Finally, the step-length is calculated using the formula:

$$L = (\Omega_c L) \cdot V_x / \omega_c \qquad (6)$$

where: L = step length of the road

Ω_c = cutoff frequency

V_x = vehicle forward velocity

ω_c = cutoff frequency in time

Also, with published spectral density data (Mitschke, 1984) the variance of the road slopes calculated can be found as a function of vehicle forward velocity.

$$\sigma^2_{z'} = (2\pi S_{z'}(0))/L \qquad (7)$$

where: $S_{z'}(0)$ = zero frequency amplitude of the roadslope spectral density

Thus, the roadway profile can be generated as a gaussian distributed random number (Dodds and Robson, 1973) with a mean value of zero and a variance as calculated above in equation (7). The distance traveled between each new slope is given above in equation (6) and the time interval over which this occurs is obtained by dividing the value of L by the vehicle forward velocity.

Simulation Results

For the first simulation, the suspension parameters shown in Table 1 were used. Also, typical initial heights of .3 m (.98 ft) and .68 m (2.23 ft) were assumed for the unsprung and sprung masses, respectively. For a vehicle forward velocity of 17.78 m/s (40 mi/h), the roadway profile shown in Fig. S-1 was obtained. The profile was created for 60 seconds with time labeled along the x-axis versus displacement of the road surface relative to an initial zero datum given in meters along the y-axis. The change in the road height over time represents the input velocity of the roadway acting on the quarter car model. Fig. S-2 shows the positions of the sprung and unsprung masses relative to the roadway versus time. For this simulation run, the active damping coefficient was set to zero. The simulation was carried out for 10 seconds with time labeled along the x-axis and the absolute height with respect to initial postion in meters labeled along the y-axis. The top curve in the graph represents the sprung mass, while the middle and bottom curves represent the positions of the unsprung mass and road height with time, respectively. Particularly evident in the figure are the relative frequencies of the three curves. The unsprung mass, as predicted by theory, has a frequency content about an order of magnitude greater than the sprung mass. Also, the unsprung mass can be seen to respond very closely to the profile of the roadway.

Fig. S-3 represents the same conditions as Fig. S-2 however this time the active damping coefficient is set equal in magnitude to the passive damping coefficient. This is the case of force controlled damping with Ba = Bp. Now, whenever the relative velocity and the sprung mass velocity are of the same sign, there will be an extra controlled damping force in addition to the passive damping force. By comparing the change in position of the sprung mass for the two figures, the effect of the force controlled semi-active force can be easily seen. The additional controlled force effectively further attenuates the transmission of road input velocity to the sprung mass. This correlates directly to less heave movement of the vehicle, or isolation of the vehicle from the road surface which leads to a more comfortable ride. The extra force appears to have little effect on the unsprung mass.

Fig. S-4a shows the effect of variation of the active damping coefficient on the attenuation of the sprung mass velocity. Again, time in seconds is labeled along the x-axis for a sample time of 10 seconds. The y-axis represents the position of the sprung mass in meters. Each of the different lines represents a different value of active damping coefficient from zero for the solid line to 4 times the passive damping coefficient for the line labeled Ba=4*Bp. The lines labeled Ba=1*Bp, Ba=2*Bp, and Ba=3*Bp represent values of active damping coefficient of 1, 2, and 3 times the passive damping coefficient. There is a very noticeable difference in the change of position over time between the curve which represents zero active damping coefficient and the curve which represents an active damping coefficient of one (Ba=1*Bp) times the passive damping coefficient. In general the graph shows the trend that with increased force controlled semi-active damping, a smoother ride in terms of vehicle body velocity is obtained. The biggest advantage is gained in the jump between the first two curves while the advantage realized between the active damping coefficients of three (Ba=3*Bp) and four (Ba=4*Bp) times the passive damping coefficient is relatively small.

Fig. S-4b shows the effect of the same variation of the active damping coefficient on the unsprung mass velocity. As seen from the fact that all of the lines fall very closely to one another, the unsprung mass position is not nearly as affected by the change in damping as was the sprung

mass position. However, because the unsprung mass position is virtually unchanged over time, there is a very important conclusion that can be drawn. Because the sprung mass position is considerably attenuated upon further increase of active damping rate and unsprung mass position is virtually unaffected, it can be concluded that suspension travel, and relative velocity across the suspension are both attenuated with the increase in active damping rate. This is a very important result as both of these factors are considered as indicators of ride comfort.

As mentioned earlier, one of the primary purposes of running the computer simulation aside from obtaining some feel for the dynamic response of the system, was to get an idea of the magnitude of the actuator forces that would be required with the control strategy. Fig. S-5 shows the variation of the actuator force over time for the condition where the active damping coefficient is four times the passive damping coefficient. For the system parameters of the typical suspension listed in Table 1, the actuator force ($Ba \cdot V1$) varies between zero and approximately 2500 N (562 lb). Finally, in order to choose correctly an actuator for the experimental test rig to verify the simulation results, suspension system values as used in Redfield, 1992 for the same test rig were used in the simulation. Those test rig values are listed in Part 2 of this paper. The results for the lab set-up actuator force versus time are shown in Fig. S-6. Here, the actuator force ranges from zero to about 100 N (22.5 lb).

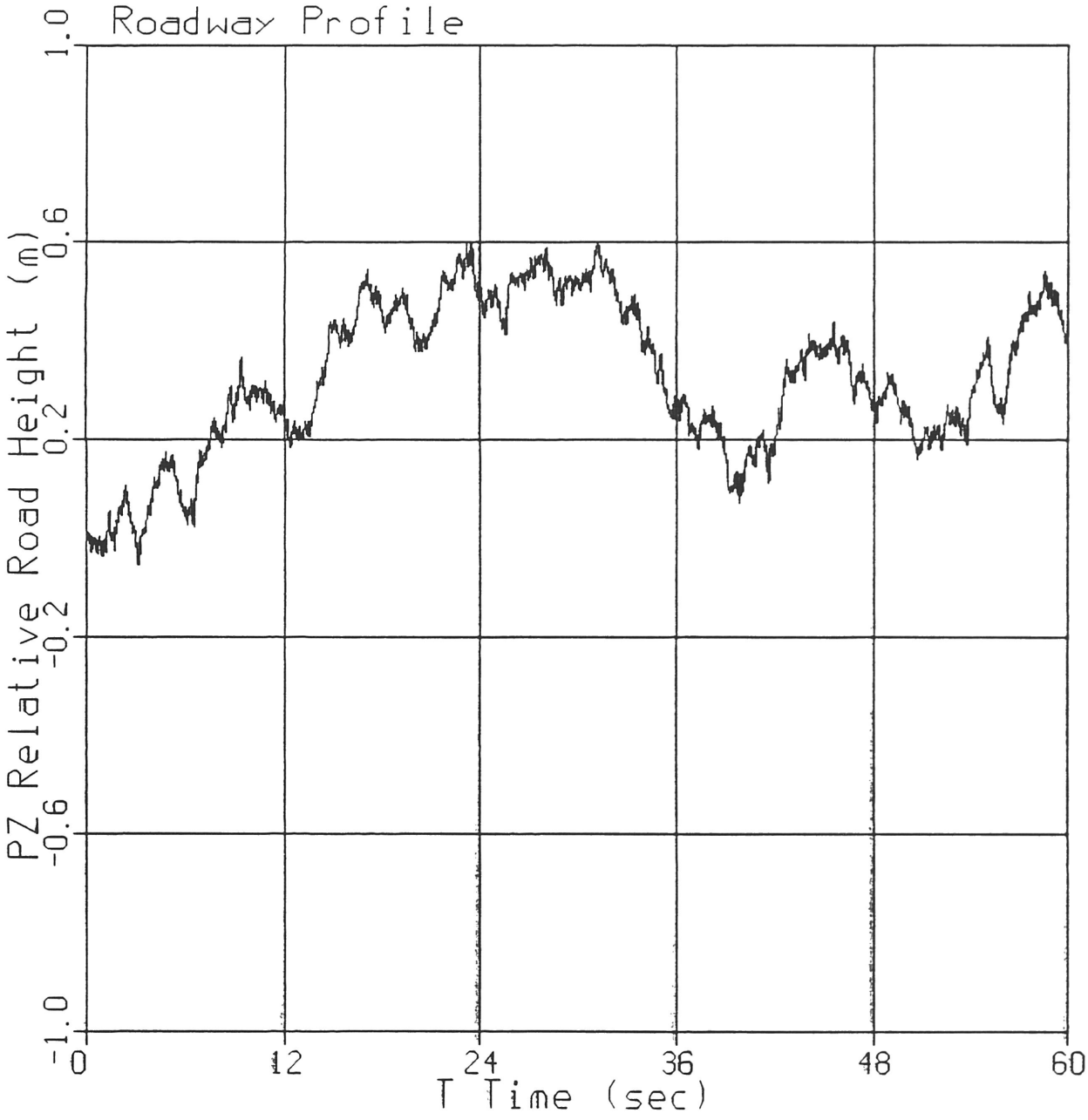

Fig. S-1 - Roadway Profile

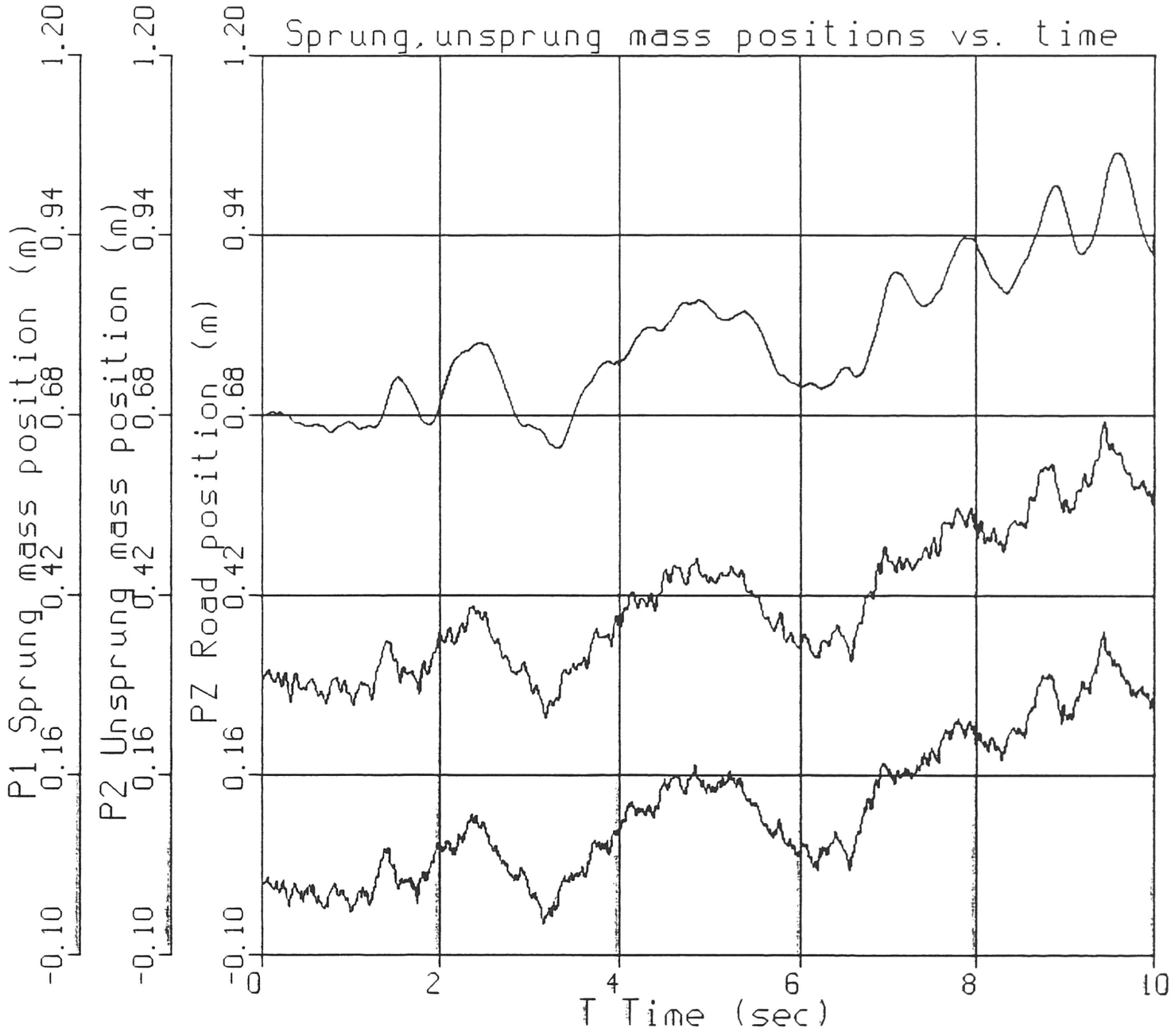

Fig. S-2 - Sprung, Unsprung mass positions vs. time

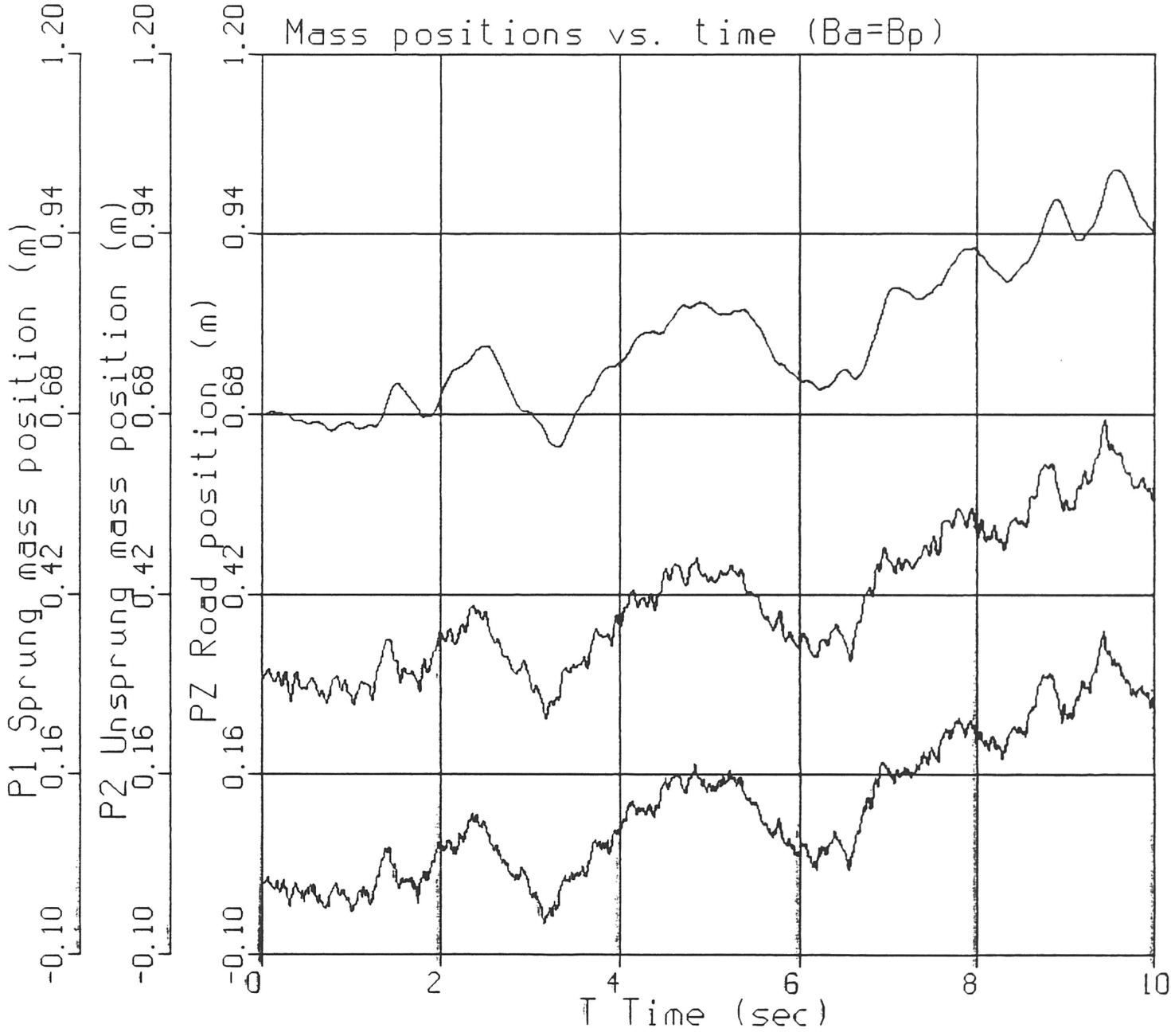

Fig. S-3 - Semi-active control with Ba = Bp

Fig. S-4a

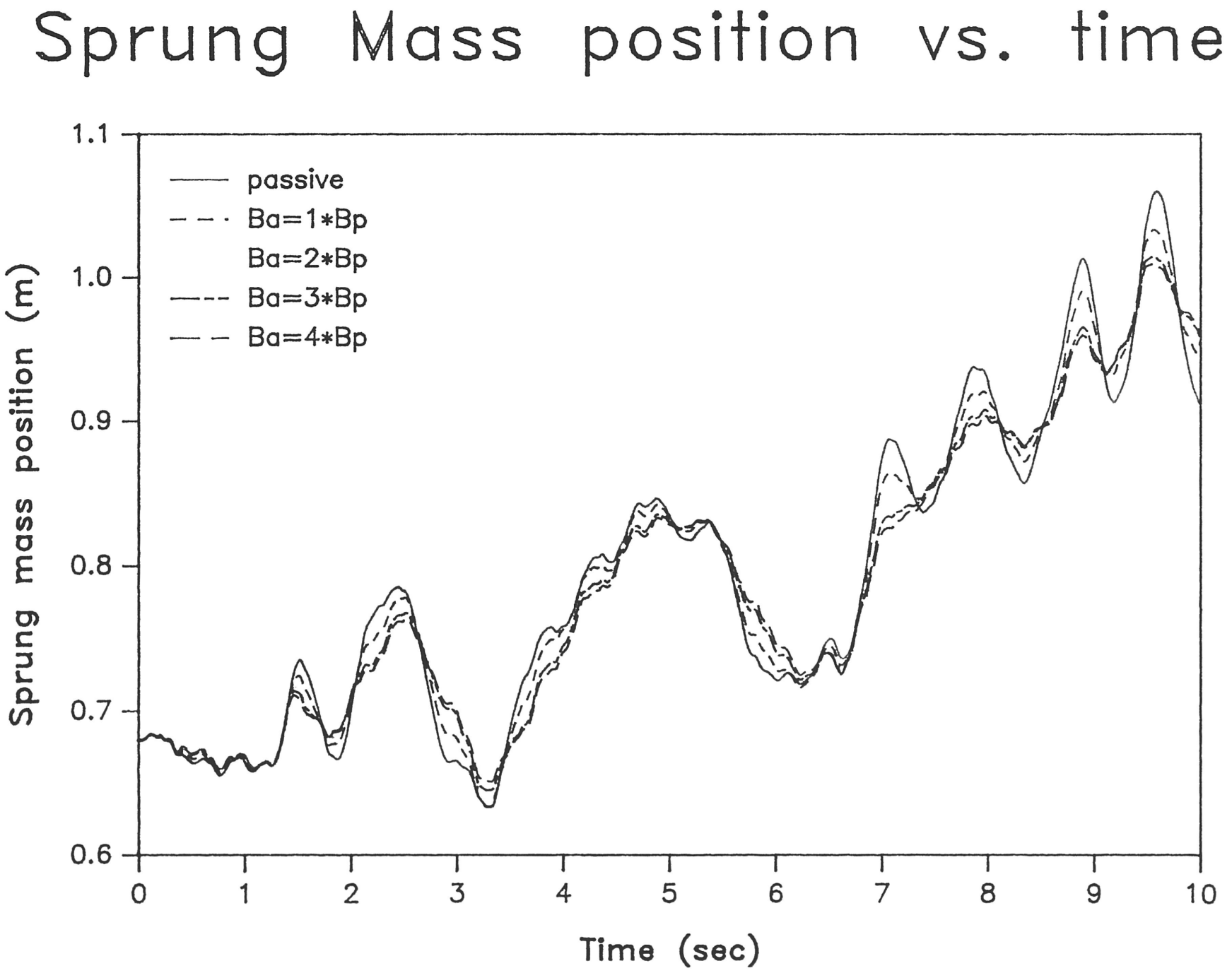
Sprung Mass position vs. time
passive
Ba=1*Bp
Ba=2*Bp
Ba=3*Bp
Ba=4*Bp
Sprung mass position (m)
1.1
1.0
0.9
0.8
0.7
0.6
0
1
2
3
4
5
6
7
8
9
10
Time (sec)

Fig. S-4b

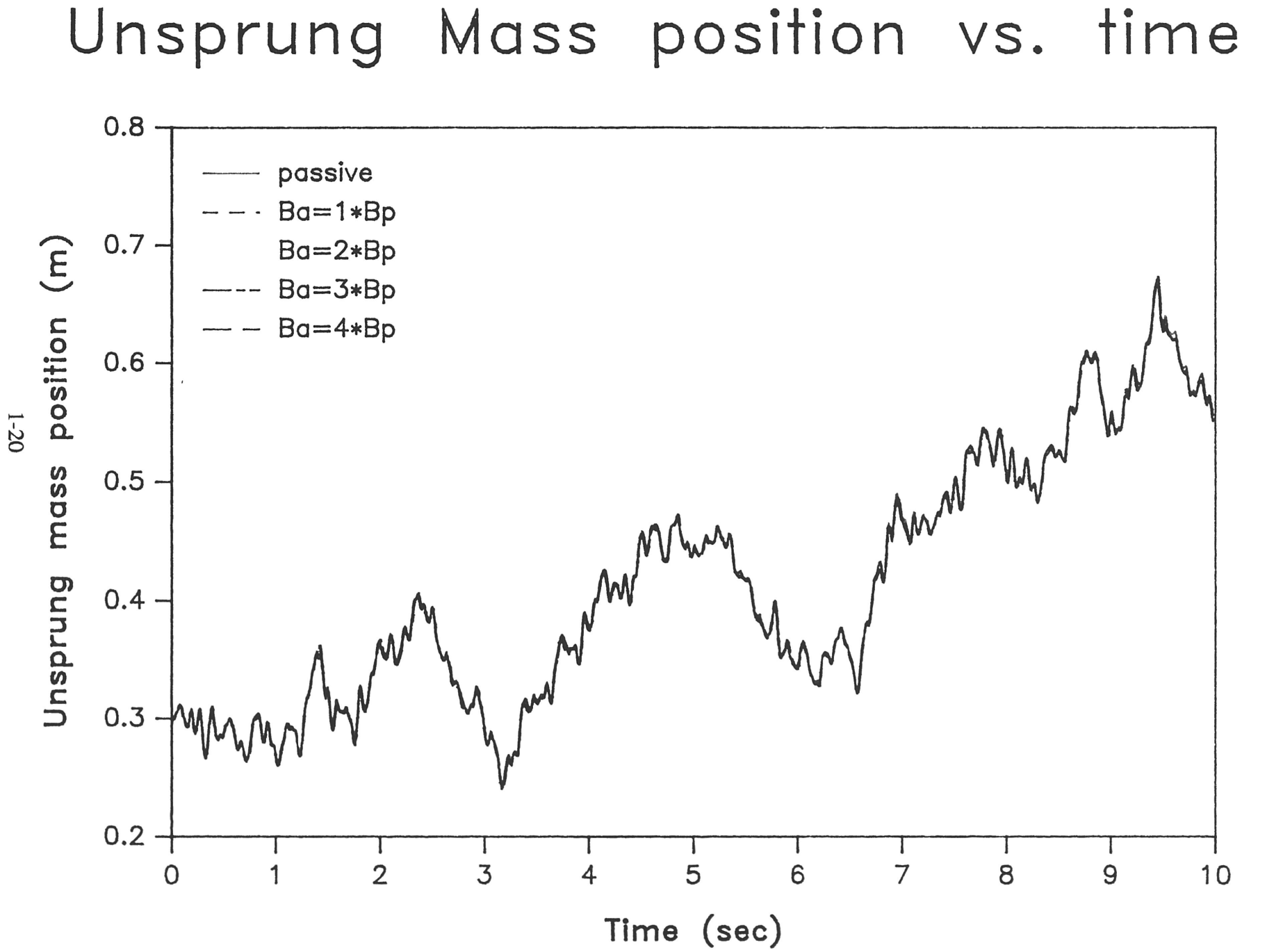
Unsprung Mass position vs. time
passive
Ba=1*Bp
Ba=2*Bp
Ba=3*Bp
Ba=4*Bp
Unsprung mass position (m)
0.8
0.7
0.6
0.5
0.4
0.3
0.2
0
1
2
3
4
5
6
7
8
9
10
Time (sec)

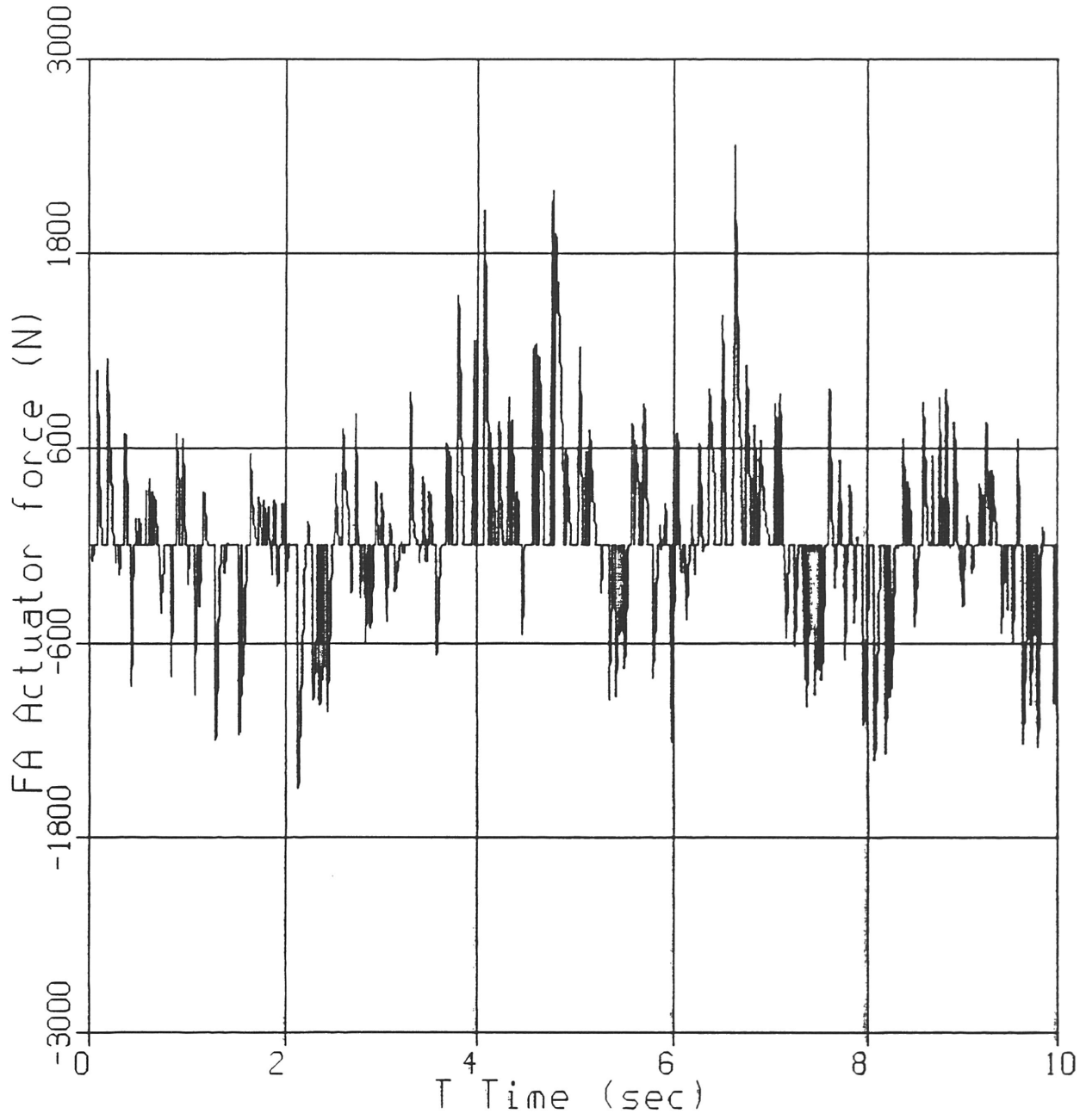

Fig. S-5 - Actuator force vs. time

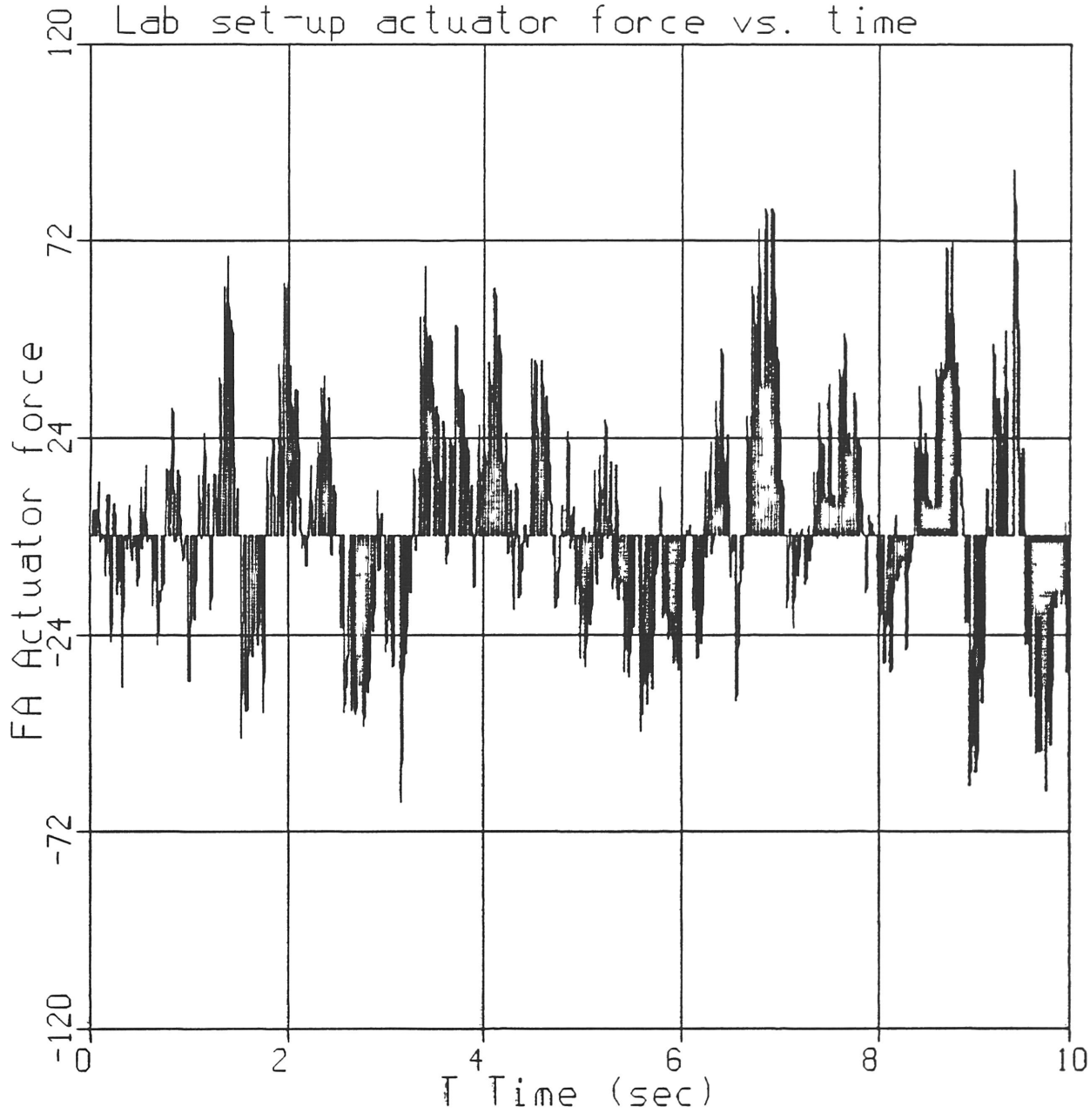

Fig. S-6 - Experimental actuator force vs. time

Part 2

EXPERIMENTAL SETUP

In order to verify the theoretical computer simulation results, a physical model representing the sprung mass and the suspension components was designed. Already in place was the air bearing table, unsprung mass, and tire spring. Because previous experimental verification of resistance controlled semi-active damping has previously been conducted on the same test rig, an attempt was made to construct as closely as possible a dynamically similar version of the force controlled semi-active apparatus so that comparison of suspension performances could be made.

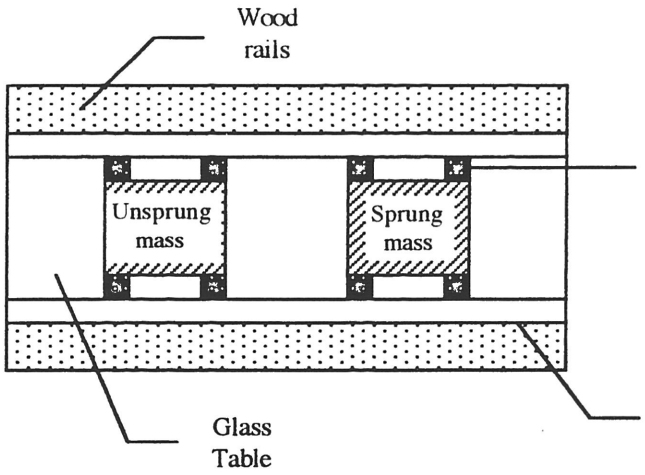

Fig. 8 - Air bearing table schematic with masses

The air bearing table is built with two aluminum rails which restrict the movement of the two experimental masses to one direction only. Both masses ride on horizontal and lateral air bearings that provide a nearly frictionless interface between the aluminum rails on the side and the glass table over which the masses ride. The sprung and unsprung masses are made with an aluminum framework and a Plexiglass bottom. The air bearings are also composed of Plexiglass and are connected to the Plexiglass bottom of the masses through a cushion pad on bottom and two small springs on the side. The side spring connections act to help center each of the masses between the two aluminum rails.

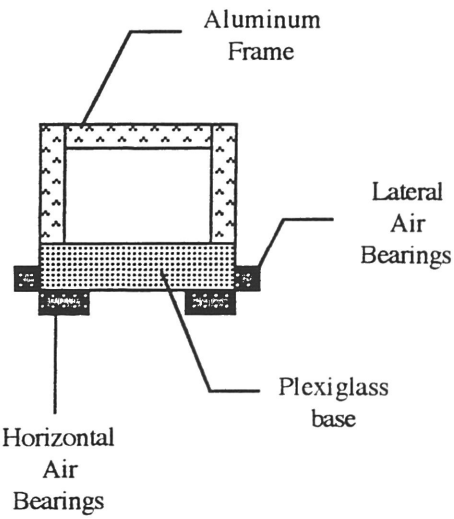

Fig. 9 - Mass schematic

The sprung mass was built with a thicker sheet of Plexiglass so that a more accurate scaling between the sprung and unsprung masses was obtained (compared to typcial

vehicle system values). The high pressure air required for the air bearings comes down from the top framework of the air bearing table in one line per mass and attached to the interior of the

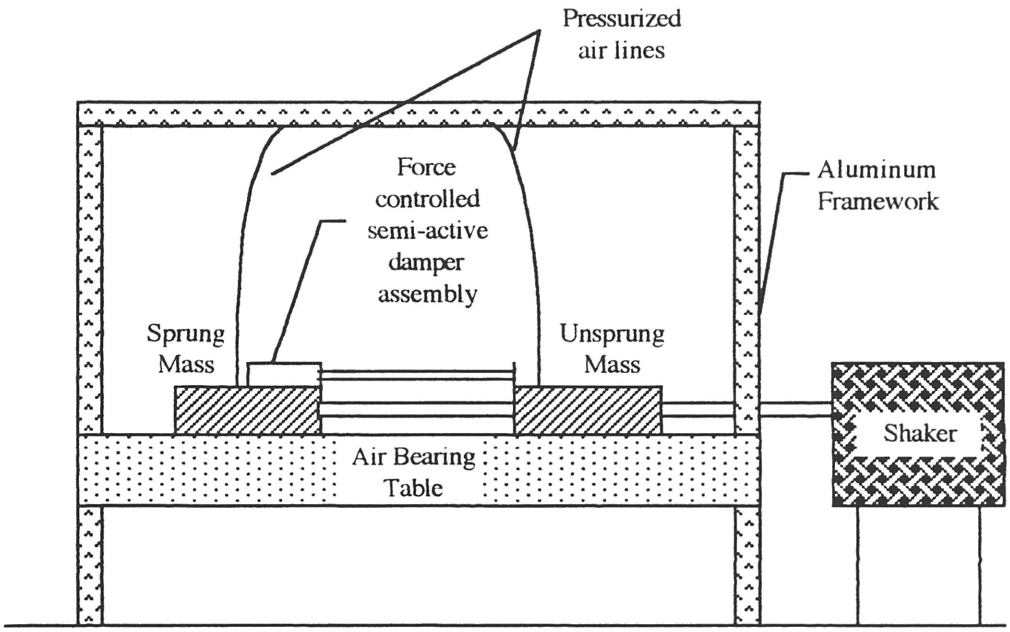

Fig. 10 - Experimental test rig set-up

framework of the masses is a splitter out of which four lines carry the pressurized air to the four corner air bearings. Also attached to the unsprung mass is a faceplate to which two dampers and the suspension spring which are built onto the sprung mass connect.

Suspension components

All of the suspension components are built onto the sprung mass and then attached to the unsprung mass as described above. The reason for this is that it helps increase the sprung-to-unsprung mass ratio which is necessary for the correct scaling to actual vehicle system values.,

In order to emulate a force controlled semi-active damping scheme, two uni-directional adjustable dampers were modified for use with two push-type solenoids. One damper/solenoid combination created the desired tensile damping force when both the relative velocity across the damper and the sprung mass velocity were positive and the other damper/solenoid combination created the need compressive damping force when the relative velocity and sprung mass velocity

were both negative.

One of the dampers provided a force while in tension, but offered little resistance, or force, in compression. The other damper operated oppositely, that is, it provided a force in compression but little in tension. Such operation was obtained with a check value built into the face of the damper piston. The dampers were modified to be adjustable by varying the position of a cylinder in the path of the airflow through the damper orifice. When the cylinder is pressed snugly against the airflow orifice with a specified force such that no airflow is allowed, the force across the damper must overcome the force applied against the cylinder in order for the cylinder to move away from the orifice and allow airflow, or relative velocity, across the damper. The force across the damper required to overcome the force exerted on the cylinder is in general not equal to the cylinder force because the piston area over which the damper force acts is much larger than the orifice area. Finally, in order to set a passive damping coefficient for the modified dampers, a rod of constant cross-section was attached to the end of the adjustable orifice cylinders and allowed to ride through the orifice at all times. This acted to reduce the orifice area by a set value resulting in increased resistance to airflow in the form of a constant Bp.

The linear actuators used to provide the force control in the semi-active damping were push-type solenoids. The solenoids were calibrated by applying different voltages across the solenoids for the same travel length and then measuring the force applied at the end of the travel.

Modified damper operation

The modified compression damper works as shown in Fig. 11. When the relative velocity across the damper is negative and the sprung mass velocity is also negative, a voltage is applied across the solenoid which produces a force equal to the product of the active damping coefficient and the sprung mass velocity, reduced by a factor of the ratio of the orifice area to the piston face area. The end of the solenoid is mated into the end of the cylinder which is pushed forward to cover the airflow orifice with the specific force. There is then no relative velocity across the damper until the

force across the damper overcomes the set actuator force at which time the damping force becomes equal to the actuator force plus a passive damping force (Bp·Vrel).

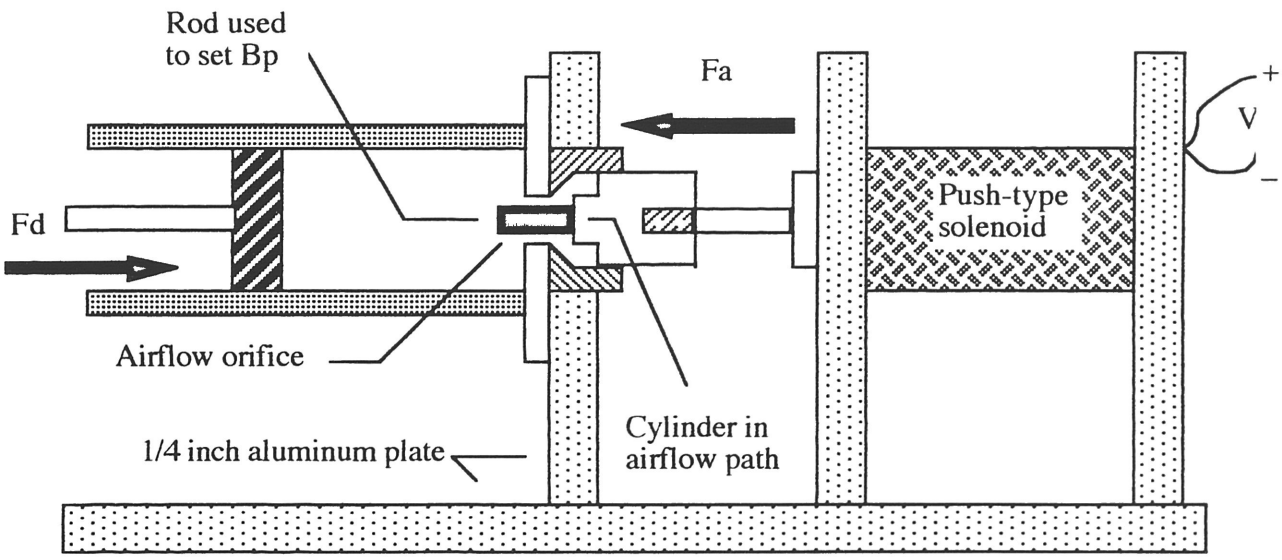

Fig. 11 - Force controlled semi-active damper for compression

The tension force control damper was constructed slightly differently. First, the solenoid direction was reversed. Also, the cylinder which fits against the airflow orifice for the tension damper had to be placed within the damper itself. Then, whenever the relative velocity across the damper is positive and the sprung mass velocity is positive, a voltage is applied to the solenoid which pulls the cylinder within the damper firmly against the airflow orifice with a force equal in magnitude to the active damping coefficient times the sprung mass velocity, reduced again by a factor of the ratio of orifice-to-piston face areas. The cylinder within the damper and the end of the solenoid are connected by a small diameter steel rod which mates into the end of the cylinder and is threaded on the other end so that it screws into the end of the solenoid, which was modified with a threaded hole. This connecting rod serves to impart to the damper a passive damping coefficient equal to that of the compression damper.

Both damper/solenoid combinations are mounted on 1/4 inch aluminum plates which mount to another 1/4 inch aluminum plate attached to the top of the sprung mass.

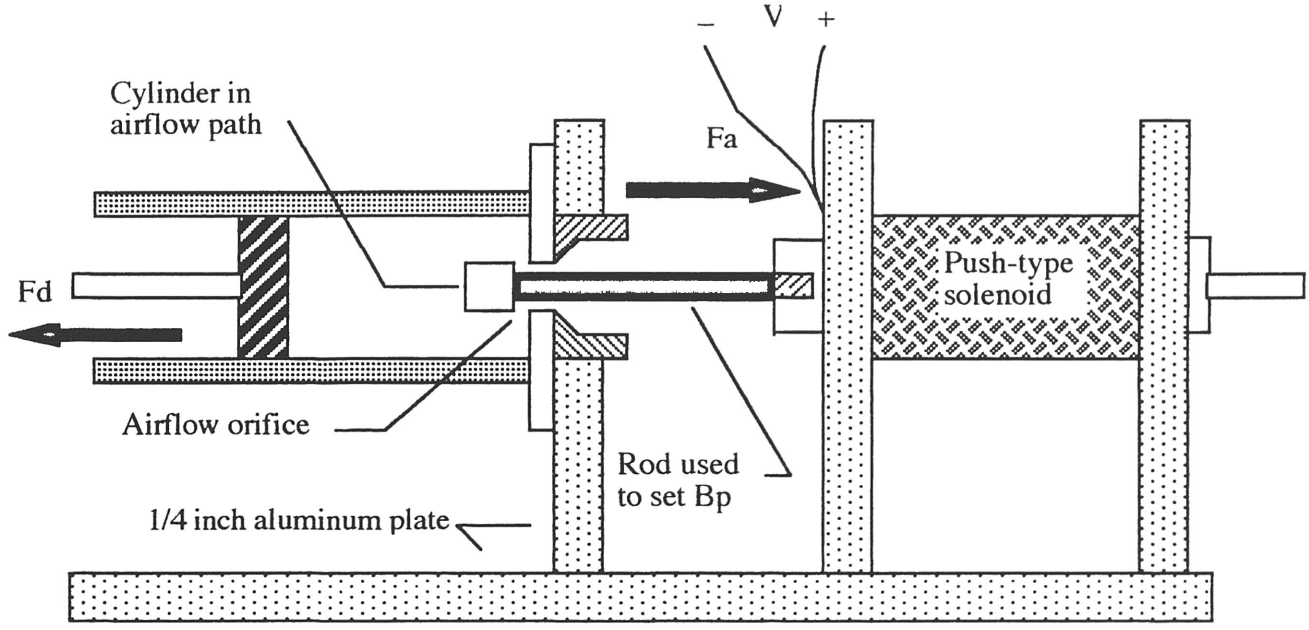

Fig. 12 - Force controlled semi-active damper for tension

The compliant nature of the suspension is modeled experimentally with an adjustable spring which is screwed onto a threaded shaft built onto the sprung mass. The spring attaches to the unsprung mass at the faceplate as described previously. The natural length of the spring can be adjusted by advancing the spring up or down the length of the threaded shaft.

Tire and road input modeling

The tire, as in the mathematical model, is modeled with an adjustable spring in the experimental setup. However, instead of screwing onto a threaded shaft as the suspension spring does, the tire spring's natural length is adjusted with the placement of a screw and washer at different positions effectively varying the number of active coils of the spring and thus the compliant nature, or spring rate, of the spring. One end of the tire spring attaches to the unsprung mass while the other is connected through the set screw to a shaft which is built onto the driving shaft of a shaker.

The shaker used in the setup is driven by a function generator. The function generator inputs a sinusoidal wave to the shaker and the shaker produces the simulated road input velocity which is a sinusoidal velocity of the same frequency as that set by the function generator. While

the road velocity input for this experimentation is of sinusoidal character, in general this does not have to be the case. A more representative road profile could be created with a computer and converted to an analog signal used to drive the shaker. However, with the sinusoidal input, frequency response of the system can be analyzed for different transfer functions and used as an analytical tool.

References

1. Crosby, M.J. and Karnopp, D.C., "The Active Damper - A New Concept for Shock and Vibration Control," 43rd Shock and Vibration Bulletin, Part H, June, 1973.

2. Dodds, C.J. and Robson, J.D., "The Description of Road Surface Roughness," *Journal of Sound and Vibration*, Vol. 31, No. 2, 1973, pp. 175-183.

3. Jenkins, G.M. and Watts, D.G., *Spectral Analysis and its Application.* Holden-Day, San Franscisco, CA, 1968.

4. Karnopp, D.C., "Active Damping in Road Vehicle Suspension Systems," *Vehicle System Dynamics*, Vol. 12, No. 6, Dec. 1983, pp. 291-312.

5. Karnopp, D.C., "Design Principles for Vibration Control Systems Using Semi-active Dampers," *Journal of Dynamic Systems, Measurement and Control*, Vol. 112, Sept. 1990, pp. 448-455.

6. Karnopp, D.C., "Force Generation in Semi-active Suspensions Using Modulated Dissipative Elements," To be published *Vehicle System Dynamics.*

7. Mitschke, M., "Fahrverhalten von PKW auf unebener Strabe," Paper #82059, *Proceedings of the XIXth International Fista Congress*, Melbourne, Australia, 1982.

8. Redfield, R.C., "Performance of Low-Bandwidth, Semi-active Damping Concepts for Suspension Control," *Vehicle System Dynamics*, Vol. 20, No. 5, 1991, pp. 245-268.

9. Redfield, R.C. and Karnopp, D.C., "Performance Sensitivity of an Actively Damped Vehicle Suspension to Feedback Variation," *Journal of Dynamic Systems, Measurement, and Control*, Vol. 111, No. 1, 1989, pp. 51-60.

10. Redfield, R.C. and Karnopp, D.C., "Roadway Elevation Profile Generation for Vehicle Simulation," *Vehicle System Dynamics*," Vol. 17, No. 5, 1988, pp. 267-280.